Temperature dependence of magnetization in ultrathin MnTe films

2000 J. Phys.: Condens. Matter 12 2913

(http://iopscience.iop.org/0953-8984/12/13/303)

J. Phys.: Condens. Matter **12** (2000) 2913–2924. Printed in the UK PII: S0953-8984(00)08329-6

Temperature dependence of magnetization in ultrathin MnTe films

R Świrkowicz

Institute of Physics, Warsaw University of Technology, Koszykowa 75, 00-662 Warsaw, Poland

E-mail: renatas@if.pw.edu.pl

Received 1 October 1999, in final form 16 December 1999

Abstract. Spin waves and the temperature dependence of local magnetization are investigated in ultrathin MnTe(100) films with antiferromagnetic ordering of type III. Calculations are performed within the framework of the Heisenberg model with use of the Green function formalism. At a given temperature the local magnetization is calculated in a self-consistent way. The influence of parameter changes in thin films (exchange integrals, anisotropy constants) on the energy spectrum, local magnon density of states and local magnetization is investigated. The obtained results strongly depend on values of exchange integrals whereas the influence of changes in anisotropy constants is very weak. When the integrals in the growth direction are lower than in-plane values the temperature dependence of the mean magnetization does not strongly depend on the film thickness in consistency with experimental data.

1. Introduction

Recently, MnTe films as well as MnTe/ZnTe, MnTe/CdTe superlattices have been investigated using neutron diffraction [1, 2] and Raman spectroscopy [3] methods. MnTe films of thicknesses of the order of micrometres prepared by means of the MBE technique show fcc crystallographic structure. Long-range antiferromagnetic order of type III (see figure 1) occurs in bulklike films as well as in ultrathin ones consisting of several monolayers. Antiferromagnets with the Heisenberg-type exchange coupling between the nearest neighbours are highly frustrated. The long-range ordering in such systems can be stabilized by an antiferromagnetic coupling between next-nearest neighbours [4]. Detailed neutron scattering measurements performed on bulklike MnTe films revealed the presence of three types of domain configuration in which AF sheets are perpendicular to the appropriate crystalline axes [2, 5–8]. An asymmetry in the domain population was observed. Domains with AF sheets perpendicular to the film surface appear to be dominant. There are two equivalent types of such domains. A fraction of the sample volume corresponding to these two types of domain is temperature dependent and increases with a decrease of temperature [6, 7]. A different situation takes place in ultrathin films. Measurements performed on superlattices containing several MnTe layers in an elementary unit show that in such systems only domains with AF sheets parallel to the surface are present [2]. According to Giebultowicz [2, 8] this preference is a direct consequence of the strain. Strain in the superlattices, in which MnTe layers are tetragonally distorted, also strongly influences the temperature dependence of the magnetization [2, 8]. Experimental data show that the magnetization closely follows the Brillouin function corresponding to a Néel temperature equal to 88 K. In MnTe/ZnTe superlattices the second-order phase transition takes

0953-8984/00/132913+12$30.00

place [2]. On the other hand, neutron diffraction measurements performed on bulklike MnTe epilayers show that the character of the temperature dependence of the magnetization changes around 60 K. An abrupt disappearance of magnetic moment is observed which probably corresponds to a change in the type of phase transition (the first-order one). According to Giebultowicz the second-order phase transition in superlattices can be a result of the strain. Experimental data obtained for superlattices also show that the magnetization curve does not essentially depend on the thickness of magnetic MnTe film. Data obtained for systems containing in an elementary unit 10 and 130 layers of MnTe follow practically the same curve [2]. It should be pointed out that in these systems effects of interlayer coupling of magnetic films through nonmagnetic ZnTe layers can be ruled out because of relatively thick nonmagnetic spacers. The exchange interlayer coupling in semiconducting heterostructures can take place only for very thin nonmagnetic spacers and was observed in MnTe/CdTe superlattices [9].

Spin-wave excitations in bulklike MnTe epilayers were investigated with the use of the Raman spectroscopy [3, 10]. A one-magnon peak was observed in the Raman spectrum taken at low temperatures. The magnon energy for the wave-vector $k = 0$ was determined and the temperature dependence of the energy was found [10]. Some results were also obtained for spin waves in MnTe/CdTe superlattices [11]. Quite recently, with the use of the inelastic neutron-scattering technique magnon excitations have been observed in bulklike fcc MnTe films and MnTe/ZnTe superlattices [6, 7, 12]. The magnon frequency determined by the neutron scattering method at the zone centre is well consistent with the value obtained from Raman measurements. Preliminary results for the spin-wave dispersion relation have been also obtained [12].

The aim of the present paper is an investigation of magnons in ultrathin MnTe films within the framework of the Heisenberg approach. Some results concerning the problem have been already published [13]. However, only the zero-temperature case with the use of spin-wave formalism has been considered. Calculations are performed within the framework of the Green function method. The temperature dependence of the magnetization in ultrathin MnTe films is found. The influence of surface parameters on the magnon density of states (DOS) and on the magnetization curve is also discussed.

2. The method

Ultrathin MnTe films of fcc structure consisting of N layers are considered. The surface is assumed to be perpendicular to the [100] direction. According to neutron diffraction studies [2] ultrathin films show the long-range AF-III type order with AF sheets parallel to the surface (figure 1). Such systems can be described with use of two equivalent magnetic sublattices [4, 13]. The Hamiltonian which includes terms corresponding to the exchange coupling, magnetocrystalline anisotropy and Zeeman interaction can be written in the form:

$$\begin{aligned} H = {} & \frac{1}{2}\sum_{l}\sum_{\delta} J_1(l, l+\delta) S_l S_{l+\delta} + \frac{1}{2}\sum_{l}\sum_{\gamma} J_2(l, l+\gamma) S_l S_{l+\gamma} \\ & + \frac{1}{2}\sum_{L}\sum_{\delta} J_1(L, L+\delta) S_L S_{L+\delta} + \frac{1}{2}\sum_{L}\sum_{\gamma} J_2(L, L+\gamma) S_L S_{L+\gamma} \\ & - g\mu_B \sum_{l} (H_0 + H_{Al}) S_l^z - g\mu_B \sum_{L} (H_0 - H_{AL}) S_L^z. \end{aligned} \tag{1}$$

Indices l and L correspond to sublattices with lattice points occupied by the localized spins aligned along the $+z$ and $-z$ axes. To describe the slab geometry in a direct way it is convenient

to introduce two indices corresponding to every lattice point $l(L)$, namely n as a layer index and $i(j)$ for in-plane vectors. The nearest- (NN) as well as the next-nearest-neighbour (NNN) couplings of antiferromagnetic type are taken into account. In the formula (1) δ denotes a vector which joins a lattice point with its NN, while γ is a vector which joins a lattice point with its NNN. The appropriate integrals are denoted by J_1 and J_2. Neutron scattering measurements show that J_1 is much greater than J_2 [14]. In ultrathin films because of stress effects the exchange integrals within atomic planes parallel to the surface and exchange integrals between two atomic planes in the direction perpendicular to the surface can be different. Moreover, changes of integrals J_1, J_2 at the surface layer can take place. All such modifications are included in the calculations. In equation (1) anisotropy effects are included in the H_A field, while H_0 corresponds to an external magnetic field. The anisotropy field H_A will have a temperature dependence characteristic of the origin of the anisotropy. The problem will be discussed later.

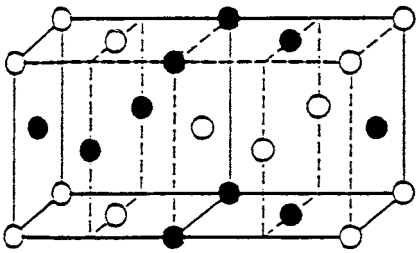

Figure 1. Elementary unit cell of the magnetic ground state of fcc MnTe (AFM structure of type III). Open and solid circles represent the localized spins aligned parallel and antiparallel to the (in-plane) z axis, respectively.

The Green function formalism is used to investigate magnons and the temperature dependence of the magnetization. Two equivalent magnetic sublattices are considered, so, two types of function are introduced: the intrasublattice Green function, G, and the intersublattice one, g. The functions are defined as follows

$$G_{nn'ii'} = \langle\langle S^+_{ni} S^-_{n'i'}\rangle\rangle \tag{2}$$

for in-plane vectors i, i' belonging to the same sublattice and

$$g_{nn'ij} = \langle\langle S^+_{ni} S^-_{n'j}\rangle\rangle \tag{3}$$

when i, j belong to different sublattices. S^+, S^- are components of the spin operator. Because of the periodic symmetry in the film plane the two-dimensional Fourier transformation can be introduced. $G_{nn'}(k)$ and $g_{nn'}(k)$ represent transforms of Green functions $G_{nn'ii'}$ and $g_{nn'ij}$, respectively. k is a wave-vector from the two-dimensional Brillouin zone.

Within the framework of the standard RPA decoupling procedure Fourier transforms of Green functions satisfy a $2N \times 2N$ matrix equation (see [15]):

$$\begin{pmatrix} \mathbf{P}_-(E) & -\mathbf{Q} \\ \mathbf{Q} & \mathbf{P}_+(E) \end{pmatrix} \begin{pmatrix} \boldsymbol{G} \\ \boldsymbol{g} \end{pmatrix} = \begin{pmatrix} \boldsymbol{M} \\ \mathbf{0} \end{pmatrix}. \tag{4}$$

In the above equation $\boldsymbol{M}$ corresponds to a N-dimensional vector with components $2\langle S_n\rangle\delta_{nn'}$, where $\langle S_n\rangle$ denotes the sublattice magnetic moment in the nth layer. In the absence of the external magnetic field it can be assumed: $\langle S_n\rangle = \langle S_{ni}\rangle = -\langle S_{nj}\rangle$. $\boldsymbol{G}$ and $\boldsymbol{g}$ are vectors corresponding to Green functions $G_{nn'}(k)$ and $g_{nn'}(k)$, respectively. E denotes the spin-wave

energy. In equation (4) **P** and **Q** represent $N \times N$ matrices determined as follows

$$\mathbf{P} = \begin{pmatrix} E-A_1 & -x_1 & 0 & \cdot & \cdot & \cdot & \cdot & 0 \\ -x_2 & E-A_2 & -x_2 & 0 & \cdot & \cdot & \cdot & 0 \\ 0 & -x_3 & E-A_3 & -x_3 & 0 & \cdot & \cdot & \cdot \\ \cdot & \cdot & \cdot & \cdot & \cdot & \cdot & \cdot & \cdot \\ \cdot & \cdot & \cdot & \cdot & \cdot & \cdot & \cdot & \cdot \\ \cdot & \cdot & \cdot & \cdot & \cdot & \cdot & \cdot & 0 \\ \cdot & \cdot & \cdot & \cdot & \cdot & \cdot & \cdot & -x_{N-1} \\ 0 & \cdot & \cdot & \cdot & \cdot & 0 & -x_N & E-A_N \end{pmatrix} \tag{5}$$

$$\mathbf{Q} = \begin{pmatrix} d_1 & x_1 & y_1 & \cdot & \cdot & \cdot & \cdot & 0 \\ x_2 & d_2 & x_2 & y_2 & \cdot & \cdot & \cdot & 0 \\ y_3 & x_3 & d_3 & x_3 & y_3 & \cdot & \cdot & \cdot \\ \cdot & \cdot & \cdot & \cdot & \cdot & \cdot & \cdot & \cdot \\ \cdot & \cdot & \cdot & \cdot & \cdot & \cdot & \cdot & \cdot \\ \cdot & \cdot & \cdot & \cdot & \cdot & \cdot & \cdot & y_{N-2} \\ \cdot & \cdot & \cdot & \cdot & \cdot & \cdot & \cdot & x_{N-1} \\ 0 & \cdot & \cdot & \cdot & \cdot & y_N & x_N & d_N \end{pmatrix}. \tag{6}$$

$\mathbf{P}_+(E)$ is obtained from $\mathbf{P}_-(E)$ after changes of all minus signs for plus signs. The detailed expressions for matrix elements can be deduced on the basis of formulas given in our earlier paper [13] (equations (13)–(22)). However, in the present case the matrix elements depend on the layer magnetization $\langle S_n \rangle$ instead of spin S. The equation (4) can be solved numerically in a self-consistent way. Green functions $G_{nn'}(k, E)$ can be calculated in a way similar to the one outlined by Diep *et al* [16].

The temperature dependence of the layer magnetization is calculated in a self-consistent way according to the formula [17, 18]

$$\langle S_n \rangle = \frac{(S+1+\Phi_n)\Phi_n^{2S+1} + (S-\Phi_n)(1+\Phi_n)^{2S+1}}{(1+\Phi_n)^{2S+1} - \Phi_n^{2S+1}}. \tag{7}$$

S denotes spin equal to $5/2$ in the MnTe case. Φ_n is expressed by G_{nn} similarly as in [17].

Now, we discuss anisotropy effects which in the Hamiltonian (1) have been represented by means of an effective field H_A. Experimental investigations show that anisotropy energy in MnTe systems is rather small as compared to the exchange one [2]. In relations in which the exchange plays an important role, the anisotropy energy can be described in an approximate way. So, the origin of the anisotropy is not discussed in this paper. It seems to us that in systems under consideration the relation $H_A = K\langle S \rangle / S$, where K is a temperature independent constant, can be assumed. To test this approximation the single-ion anisotropy is also considered. In such a case instead of H_A the following terms should be introduced into Hamiltonian (1)

$$-D\left[\sum_l (S_l^z)^2 + \sum_L (S_L^z)^2\right] \tag{8}$$

where D is a temperature independent parameter. The basic Green functions $\langle\langle S_{ni}^+; S_{n'i'}^- \rangle\rangle$, $\langle\langle S_{ni}^+; S_{n'j}^- \rangle\rangle$ can still be evaluated following the procedure described earlier, except that in addition to the usual RPA decoupling

$$\langle\langle S_{n''l''}^z S_{ni}^+; S_{n'i'}^- \rangle\rangle \to \langle S_{n''}^+ \rangle \langle\langle S_{ni}^+; S_{n'l'}^- \rangle\rangle \tag{9}$$

it is now also necessary to assume the decoupling of the form

$$\langle\langle S_{ni}^z S_{ni}^+ + S_{ni}^+ S_{ni}^z; S_{n'i'}^- \rangle\rangle \to 2p_n \langle S_n \rangle \langle\langle S_{ni}^+; S_{n'i'}^- \rangle\rangle \tag{10}$$

for Green functions involving a product of operators at the same site. The decoupling scheme of the above form was profoundly discussed in reference to the Heisenberg Hamiltonian with single-ion anisotropy in bulk materials [19, 20]. We adapt the approach to the case of thin films. A similar approach was also used for metamagnetic thin films [21, 22]. Following the decoupling procedure employed by Lines [19] and by Anderson and Callen [20] one can express p_n in the form:

$$p_n = [3\langle (S_n^z)^2\rangle - S(S+1)]/2\langle S_n\rangle \qquad \text{Lines decoupling} \tag{11}$$

$$p_n = 1 - \left(\frac{1}{2S}\right)^2 [S(S+1) - \langle (S_n^z)^2\rangle] \qquad \text{Anderson–Callen decoupling.} \tag{12}$$

At non-zero temperatures it is possible to calculate $\langle (S_n^z)^2\rangle$ self-consistently in the way employed by Callen [18] or using a theorem by Callen and Strickmann [23] one can relate $\langle (S_n^z)^2\rangle$ to the sublattice magnetization $\langle S_n\rangle$.

Following the outlined decoupling procedure the final results for the Green functions can be written in the same form as previously, however with the effective field H_A given in the form:

$$g\mu_B H_A = 2p\langle S\rangle D. \tag{13}$$

In the next section numerical results are presented and the influence of anisotropy terms on the temperature dependence of the sublattice magnetization is discussed.

3. Results

Numerical calculations are performed for MnTe films with (100) symmetry consisting of $N = 5$–15 monolayers. Values of exchange integrals are taken from neutron diffraction measurements, namely $J_1 = 9.73$ cm^{-1}, $J_2 = 1.07$ cm^{-1} [14]. They correspond to bulk materials. The anisotropy field is estimated on the basis of Raman scattering data obtained for the zero wave-vector magnons in epitaxial MnTe films at low temperatures [3]. It gives $H_A(T = 0) = 3.25\ T$. To compare results obtained with different approaches to anisotropy terms the temperature dependence of the sublattice magnetization is calculated for a film consisting of $N = 7$ ML. The bulk parameters are taken. In figure 2 the mean value of the sublattice magnetization $\langle S\rangle = 1/N \sum \langle S_n\rangle$ is depicted for the simple case with $H_A = K\langle S\rangle/S$ and for the single-site anisotropy with decoupling approximations introduced by Lines (equation (11)) and by Anderson and Callen (equation (12)). It can be seen that in a wide temperature region (practically up to 60 K) the results do not depend strongly on the assumed approximation. The more important deviations can appear in the vicinity of T_N; however, it is difficult to obtain self-consistent solutions for $\langle S\rangle$ at temperatures close to T_N (see also [16]). So, it seems to us that in systems under consideration the simple form of anisotropy $H_A = K\langle S\rangle/S$ can be taken and the results which will be presented are obtained within the framework of this approach.

In ultrathin systems changes of parameters can take place. As stated earlier ultrathin MnTe films are strained which can lead to a difference between values of exchange integrals in the growth direction and exchange integrals within atomic planes parallel to the film surface. Some changes in anisotropy field and exchange integrals can also take place at the surface or interface. However, to our knowledge, there are no reliable data concerning the changes of exchange integrals or anisotropy fields in ultrathin MnTe films. Therefore, numerical calculations are performed here for a series of different values of parameters and the influence of the changes on spin-wave energies, local DOS and local magnetization is discussed. First of all, values of parameters (exchange integrals, anisotropy constant) are changed in the surface layers,

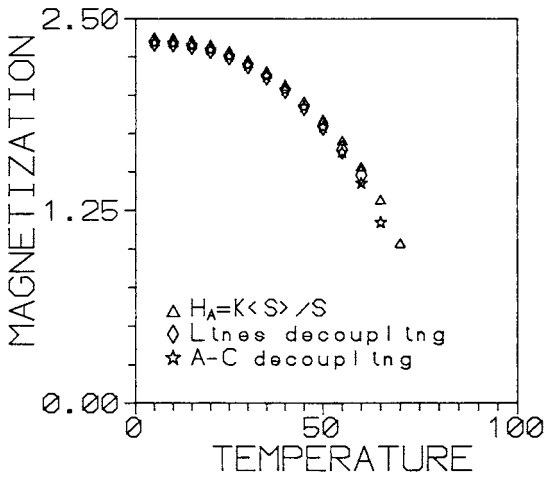

Figure 2. Temperature dependence of the mean magnetization calculated for a film consisting of $N = 7$ ML with different approximations for the anisotropy term (see text). Bulk values of parameters are taken.

whereas for inner planes bulk parameters are assumed. Next, exchange integrals between two layers $J_\perp$ are assumed to be different from those within atomic planes $J_\parallel$ (equal to bulk).

3.1. Spin-wave energies and magnon density of states

At first, the influence of the parameters on the magnon spectrum and local DOS is investigated. The energies of spin-wave modes calculated for the film consisting of seven layers are depicted in figure 3. Solid lines represent dispersion curves of seven modes which can propagate in the film plane in the [010] direction. All parameters are assumed to be equal to their bulk values. Additionally, curves corresponding to the mode with the lowest energy obtained for different parameters, namely $K_S = 0.5K$, $J_{1S} = 0.75J_1$ and $J_\perp = 0.75J_1$ are given. One can see that changes of exchange integral J lead to rather strong modifications of spin-wave energies. On the other hand, the influence of the surface anisotropy is minor. An influence of J on spin waves in thin films with AF order was also pointed out by Stamps and Camley [24]. According to figure 3 one can see that in the region of high values of k-vector the dispersion curves corresponding to different modes are at certain points very close to one another displaying interactions. The results to some extent are similar to the ones obtained in [24] for coupled dipole-exchange modes in antiferromagnetic films; however, in the present case the curves do not cross. According to figure 3 one can also see that spin-wave spectrum is strongly influenced by temperature; however, changes of parameters lead to similar modifications as at low temperatures.

The density of states in the layer n is determined by the imaginary part of the Green function. The calculated DOS strongly depends on the layer index and values of parameters. For $J_{1S} = J_1$ the surface density of states in the range of low energies is essentially smaller than for interior layers (figure 4: the solid line represents the DOS of the surface layer and the long-dashed line the DOS of the central plane). However, the surface DOS calculated for $J_{1S} = 0.75J_1$ is much higher than for the previous case. It can be expected that for $J_{1S} = 0.75J_1$ spin waves will influence the surface magnetization rather strongly.

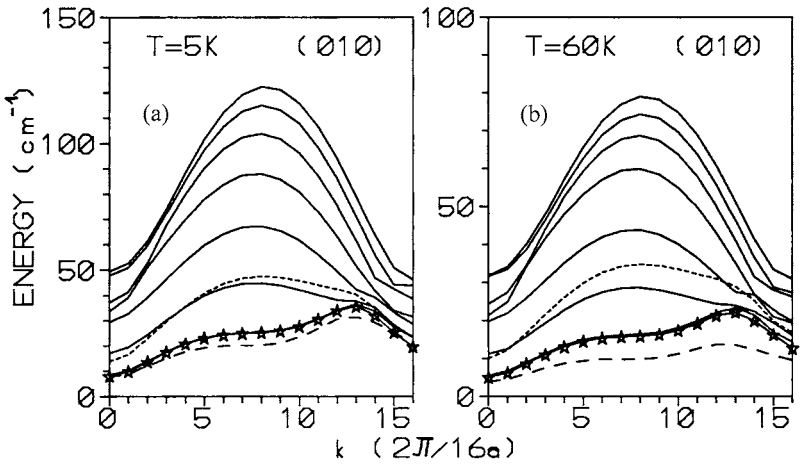

Figure 3. Magnon dispersion relations in MnTe films consisting of $N = 7$ layers calculated for $J_{1S} = J_1$, $K_S = K$ (solid lines, all modes are given), $J_{1S} = 0.75J_1$, $K_S = K$ (dashed lines), $J_\perp = 0.75J_1$, $J_{1S} = J_1$, $K_S = K$ (dotted lines), $K_S = 0.5$ K, $J_{1S} = J_1$ (asterisks). For cases with modified parameters only one mode with the lowest energy is presented. (a) and (b) correspond to $T = 5$ and 60 K, respectively.

3.2. Local magnetization

The local magnetization of the system under consideration is calculated with the use of equation (4). At low temperatures self-consistent results are achieved in a few iteration steps, but it is difficult to obtain the solutions for temperatures close to T_N.

Profiles of the magnetization calculated for $T = 5$ K and 60 K and for different values of parameters are presented in figure 5. It can be seen that at low temperatures oscillations of the local magnetization are obtained. In all cases the lowest moment corresponds to the subsurface layer. A strong decrease of the anisotropy constant at the surface leads to a decrease of the surface magnetization but the subsurface moment is still lower. A similar result was obtained by Diep for antiferromagnetic thin films [25]. For values of J_{1S} lower than $0.5J_1$ no self-consistent solutions are obtained even at $T = 5$ K, which indicates that the assumed AFIII ordering is not stable. In the case of films thinner than 9 ML the influence of surfaces is more important and no solutions are found unless $J_{1S} \geqslant 0.75J_1$.

At high temperatures magnetization profiles strongly depend on the values of the parameters. For $J_{1S} = J_1$ the surface magnetization is still slightly higher than the central layer one. This may well be the effect of the very flat dispersion relation of low-lying modes in the region of the middle values of the wave-vector k. These modes influence the magnetization of the inner layers very strongly; however, their amplitudes at the surface are low. A quite different situation takes place for $J_{1S} = 0.75J_1$. In this case the magnon spectrum is shifted towards lower energies and moreover the amplitudes of low-energy modes are the highest at the surface. These two effects influence the magnetization curve very strongly especially at the surface. Therefore, the surface magnetization decreases very fast with temperature and according to figure 6 the decrease is practically linear in a wide region of temperatures. On the other hand, when $J_\perp = 0.75J_1$ ($J_{1S} = J_1$) the magnetization curve does not depend strongly on the layer index; the surface and central layer moments decrease approximately in the same way. The decrease certainly is not linear. Therefore, in systems under consideration the local magnetization strongly depends on values of parameters.

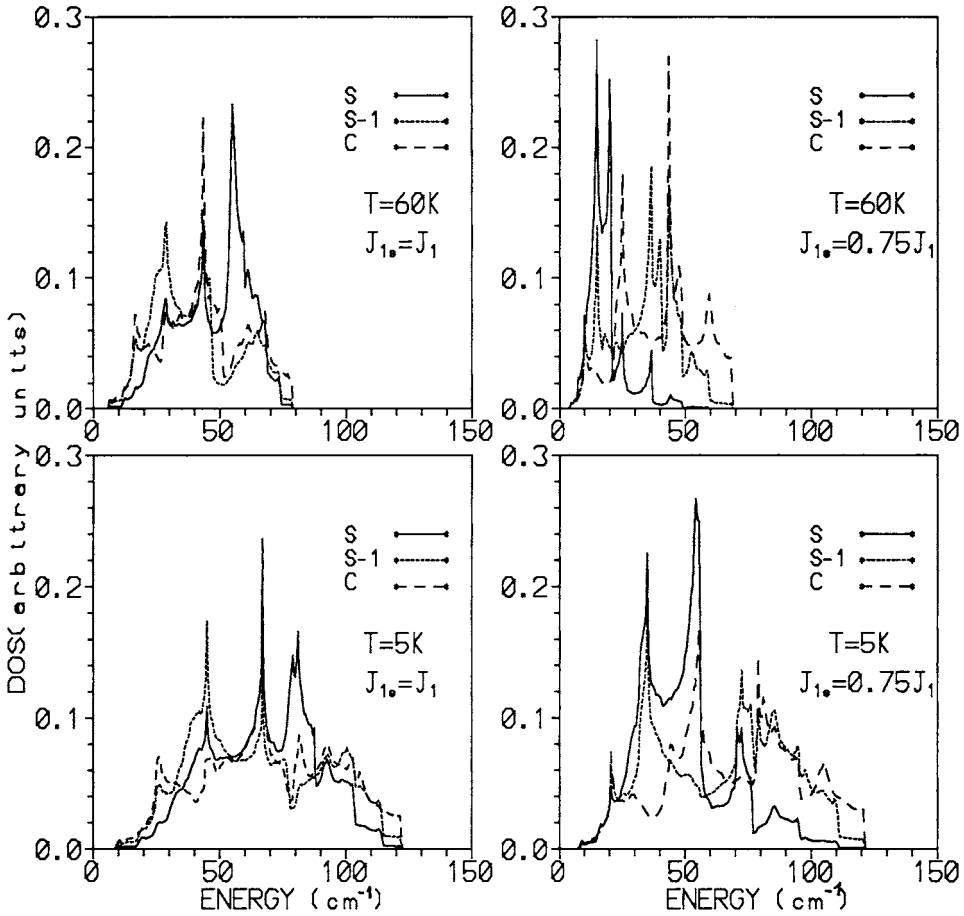

Figure 4. Local DOS calculated for surface (s), subsurface (s − 1) and central (c) layers with two sets of parameters: $J_{1S} = J_1$, $K_S = K$; $J_{1S} = 0.75J_1$, $K_S = K$ at $T = 5$ and 60 K. $N = 7$ is assumed.

In figure 7 temperature dependences of the mean magnetization of the film are presented for systems of different thickness with the same values of parameters, $J_\perp = 0.75J_1$ ($J_{1S} = J_1$). It can be seen that the number of layers in the film influences the magnetization curve rather slightly. The curves corresponding to $N = 7$ and $N = 15$ are quite close to one another. It should be also pointed out that for the chosen values of parameters, namely for exchange integrals in the direction perpendicular to the surface lower than the in-plane ones ($J_\perp = 0.75J_1$) the mean magnetization of the ultrathin film (for $N \geqslant 7$ ML) can be quite close to the bulk one (figure 7). The result is well consistent with the one known from neutron diffraction measurements performed on MnTe/ZnTe superlattices with different number of magnetic layers in the elementary unit [2].

Raman measurements show that the temperature dependence of magnon energy in MnTe films follows the Brillouin curve quite well [10]. The results for magnon energy as a function of temperature in bulk fcc MnTe obtained within the framework of the Heisenberg model with RPA decoupling are also well consistent with experimental data [26]. Therefore, one can expect that in the system under consideration magnon–magnon interactions are not very

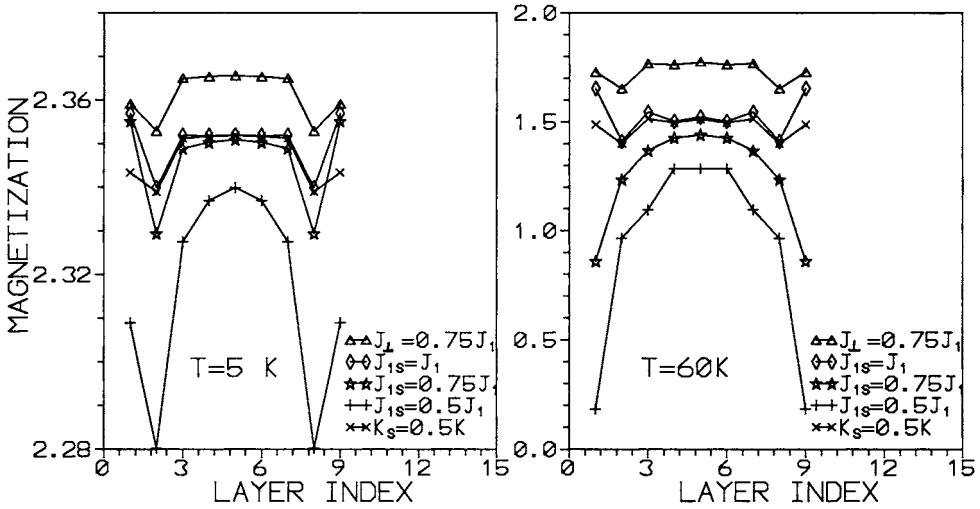

Figure 5. Magnetization profiles calculated for different sets of parameters at $T = 5$ and 60 K. Only one parameter (given in the figures) is changed in each case; other parameters are equal to bulk values.

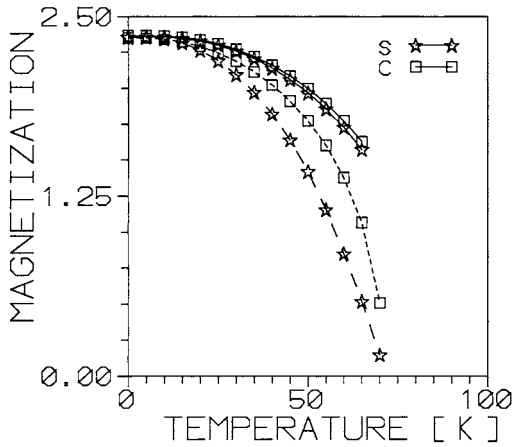

Figure 6. Temperature dependence of the surface (s) and central layer (c) magnetization calculated for films consisting of $N = 15$ layers with $J_\perp = 0.75J_1$, $J_{1S} = J_1$ (solid lines) and $J_\perp = J_1$, $J_{1S} = 0.75J_1$, (dashed lines); other parameters take their bulk values.

important and do not critically influence the magnon energy. Temperature dependences of spin-wave modes with $k = 0$ calculated for an ultrathin film with $N = 7$ layers are presented in figure 8. A decrease of magnon energies for all modes is clearly seen. When energies of the modes are normalized to their values at $T = 0$ K, the obtained curves lie very close to one another and all of them are included between surface and central layer magnetizations (also normalized to 1). In fact the normalized mean energy of magnon modes follows the curve corresponding to the mean (normalized) magnetization quite well. In figure 9 normalized mean energy of magnons calculated for a film consisting of 15 ML is presented as a function of temperature. Results found for bulk MnTe as well as experimental data obtained for bulklike films with use of Raman spectroscopy [10] are also given. One can see that in the region of

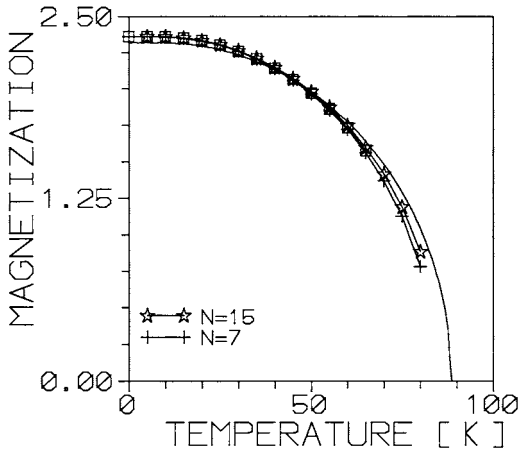

Figure 7. Temperature dependence of the mean magnetization of the film for $N = 7$ and 15 layers. $J_\perp = 0.75J_1$ ($J_{1S} = J_1$). The curve corresponding to the magnetization in bulk fcc MnTe is also given.

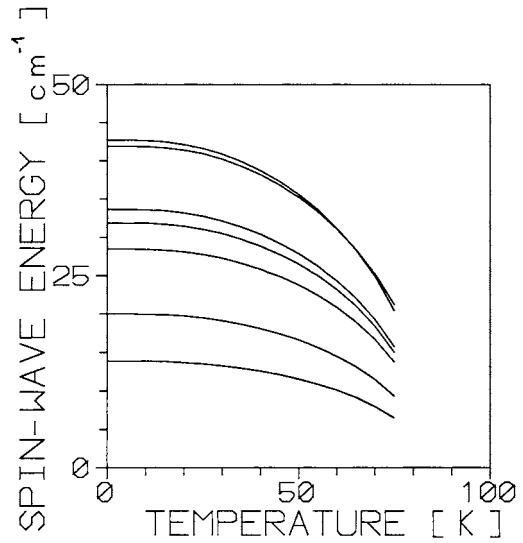

Figure 8. Temperature dependences of spin-wave modes with $k = 0$. $J_\perp = 0.75J_1$ ($J_{1S} = J_1$) and $N = 7$ are taken.

low and middle temperatures experimental points follow the curve calculated for bulk MnTe with $T_N = 88$ K. Results found for the ultrathin film with $J_\perp = 0.75J_1$, $J_{1S} = J_1$ are also quite close to the experimental data. For higher temperatures discrepancies can be expected. The problem was discussed in detail by Giebultowicz *et al* [2].

4. Conclusions

Calculations performed for ultrathin films with the use of the Green function formalism show that magnon energies and magnetization curves depend very strongly on values of exchange

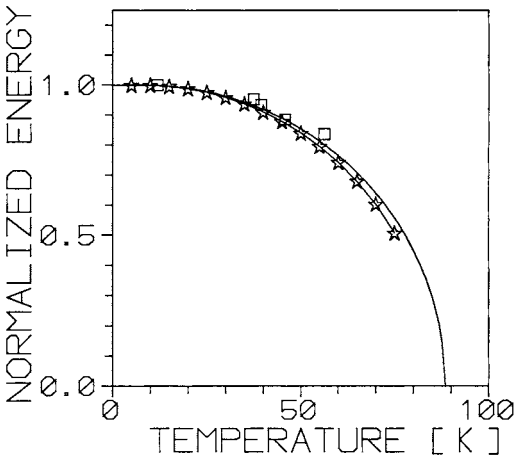

Figure 9. Temperature dependence of normalized mean energy of magnons (with $k = 0$) calculated for a film with $N = 15$ and $J_\perp = 0.75J_1$, $J_{1S} = J_1$ (asterisks). Results obtained for bulklike MnTe epilayers using Raman spectroscopy are presented (squares). The solid line corresponds to theoretical results for bulk material.

integrals. When anisotropy of J is taken into account, namely, the exchange integrals in the growth direction are lower than in-plane values, calculated results are quite close to Raman spectroscopy data at low and middle temperatures. The obtained results also seem to confirm the conclusion drawn on the basis of neutron diffraction measurements that the magnetization curve is not strongly influenced by the thickness of MnTe film.

Experimental investigations performed on MnTe/ZnTe superlattices with the use of nonelastic neutron diffraction as well as measurements using the Raman spectroscopy for MnTe/CdTe superlattices on various substrates are at present in rather a preliminary state. However, they are very promising and one can expect that very soon a more direct comparison of the experimental and theoretical data for ultrathin MnTe films will be possible.

Acknowledgment

The author is very indebted to Professor J Barnaś for helpful discussions.

References

[1] Kłosowski P, Giebultowicz T M, Rhyne J J, Samarth N, Luo H and Furdyna J K 1991 *J. Appl. Phys.* **70** 6221
[2] Giebultowicz T M, Kłosowski P, Samarth N, Luo H, Furdyna J K and Rhyne J J 1993 *Phys. Rev.* B **48** 12 817
[3] Szuszkiewicz W, Jouanne M, Dynowska E, Janik E, Karczewski G, Wojtowicz T and Kossut J 1995 *Acta Phys. Pol.* A **88** 341
[4] ter Haar D and Lines M P 1962 *Phil. Trans.* A **255** 1
[5] Qun Shen, Luo H and Furdyna J K 1995 *Phys. Rev. Lett.* **75** 2590
[6] Szuszkiewicz W, Henion B, Jouanne M, Morhange J F, Dynowska E, Janik E and Wojtowicz T 1999 *J. Magn. Magn. Mater.* **196–197** 425
[7] Szuszkiewicz W, Hennion B, Dynowska E, Janik E, Wojtowicz T and Zieliński M 1999 *Proc. 28th Int. School on Physics of Semiconducting Compounds, Jaszowiec'99* p 101
[8] Giebultowicz T M, Luo H, Samarth N, Furdyna J K, Nunez V, Rhyne J J, Faschinger W, Springholtz G, Bauer G and Sitter H 1994 *Physica* B **198** 163
[9] Nunez V, Giebultowicz T M, Faschinger W, Bauer G, Sitter H and Furdyna J K 1994 *J. Cryst. Growth* **138** 877

[10] Szuszkiewicz W, Dynowska E, Janik E, Karczewski G, Wojtowicz T, Kossut J, Jouanne M and Gębicki W 1996 *Proc. 23rd Int. Conf. on Physics of Semiconductors (Berlin, 1996)* vol 1, ed M Scheffler and R Zimmerman (Singapore: World Scientific) p 385
[11] Jouanne M, Szuszkiewicz W, Morhange J F, Kanehisa M A, Hartmann J M, Mariette H, Dynowska E, Karczewski G, Wojtowicz T, Kossut J and Barnaś J 1998 *J. Cryst. Growth* **184/185** 947
[12] Szuszkiewicz W, Hennion B, Jouanne M, Morhange J F, Dynowska E, Janik E, Wojtowicz T, Zieliński M and Furdyna J K 1998 *Acta Phys. Pol.* A **94** 583
[13] Barnaś J and Świrkowicz R 1998 *Phys. Status Solidi* b **206** 787
[14] Giebultowicz T M, Rhyne J J, Ching W Y, Huber D L Furdyna J K, Lebech B and Gałązka R R 1989 *Phys. Rev.* B **39** 6857
[15] Loison D and Diep H T 1992 *Phys. Lett.* A **162** 405
[16] Diep H T, Levy J C S and Nagai O 1979 *Phys. Status Solidi* b **93** 351
[17] Haubenreisser W, Brodkorb W, Corciovei A and Costache G 1972 *Phys. Status Solidi* b **53** 9
[18] Callen H B 1963 *Phys. Rev.* **130** 890
[19] Lines M E 1967 *Phys. Rev.* **156** 534
[20] Anderson F B and Callen H B 1964 *Phys. Rev.* **136** 1068
[21] Rudzinski W and Maciejewski W 1992 *Phys. Status Solidi* b **174** 547
[22] Rudzinski W and Maciejewski W 1993 *Phys. Status Solidi* b **175** 247
[23] Callen H B and Strickmann S 1965 *Solid State Commun.* **3** 5
[24] Stamps R L and Camley R E 1987 *Phys. Rev.* B **35** 1919
[25] Diep H T 1991 *Phys. Rev.* B **43** 8509
[26] Świrkowicz R 1997 *J. Phys.: Condens. Matter* **9** 6901